Polymer Chemistry

ROYAL SOCIETY OF CHEMISTRY

REVIEW

View Article Online
View Journal | View Issue

Cite this: *Polym. Chem.*, 2025, **16**, 396

Circularly polarized polymeric light-emitting diodes: preparation and properties

Na Wang,[a] Huli Yu,*[b] Hai Zhong,[a] Min Duan,[a] Jianping Deng *[a] and Biao Zhao*[a]

Received 27th August 2024,
Accepted 16th December 2024

DOI: 10.1039/d4py00939h

rsc.li/polymers

Organic light emitting diodes with circularly polarized luminescence (CPL) properties have attracted extensive attention owing to their significant potential in 3D displays, spintronics, encrypted data storage, and so forth. Amongst various reported CPL materials, polymer-based chiral emitters constitute an important class because of their advantages of high thermal stability, good film-forming properties, low cost and good solution processability, which are helpful in developing emission-color-adjustable, large-area and flexible photoelectric devices. In this review, we systematically summarize state-of-the-art circularly polarized polymeric light-emitting diodes (CP-PLEDs), in which different types of polymer-based emitting materials covering chiral conjugated luminescent polymers, achiral conjugated luminescent polymers doped with chiral inducers, and chiral polymer-based metal complexes are introduced. Additionally, the challenges and opportunities for the future development of CP-PLEDs are also discussed. This review article is expected to stimulate more unprecedented achievements of polymer-based CPL emitters as well as their related electroluminescent devices, further promoting their future practical applications.

1. Introduction

Polarization of light is widely present in nature, and can be divided into linearly polarized light, circularly polarized light, and elliptically polarized light, based on variation in the direction and amplitude of the light vibration.[1] Circularly polarized (CP) light refers to rotation in a single direction in which the amplitude of a light wave remains constant and the vibration direction remains constant over time, resulting in a circular motion trajectory of the end vector. Traditionally, CP light can be conveniently and continuously obtained from non-polarized light through a linear polarizer and quarter-wave plate, but this method generally suffers from serious loss of brightness and complex device architecture. In addition to this physical approach, CP light can also be directly generated from chiral luminescent materials, which is known as circularly polarized luminescence (CPL).[2–5] According to their different excitation mechanisms, CPL can be classified into CP photoluminescence (CPPL) and CP electroluminescence (CPEL). Up to now, chiral luminescent materials with CPPL have made considerable progress,[6–9] but those with CPEL properties are still in their infancy. Organic light-emitting diodes (OLEDs) are the most promising device for realizing EL, and have been widely applied in display and lighting technology.[10] When the emitter of an OLED device is replaced by a chiral luminescent molecule, CPEL could be realized efficiently and directly. In the past few years, OLEDs with CPL performance have emerged as a hot topic in multi-disciplinary fields due to their great potential in 3D displays, spintronics, optical data storage, *etc.*[11–16]

Since the first example of circularly polarized OLEDs (CP-OLEDs) was reported by Meijer *et al.* in 1997,[17] studies on CP-OLEDs have attracted increasing interest, and a growing number of CPEL emitters have been developed successively, including chiral organic small molecules, chiral organometallic complexes and chiral conjugated polymers.[18] Compared with the first two types, polymer-based CPEL emitters are highly attractive due to their merits of high stability, easy modification, and good solution processability, and are suitable for large-area and flexible devices. Nowadays, researchers have developed a series of CP polymeric light-emitting diodes (CP-PLEDs) with different colors as well as white light emission. According to their composition, polymer-based CPEL emitters can be divided into three main categories: (1) chiral conjugated luminescent polymers;[17,19,20] (2) achiral conjugated luminescent polymers doped with chiral inducers;[21–23] and (3) chiral polymer-based metal complexes.[24,25] More importantly, chiral polymers with thermally activated delayed fluorescence (TADF) features have also been designed and synthesized for CP-PLEDs in the past few years,[26–28] which is con-

[a]*State Key Laboratory of Chemical Resource Engineering, College of Materials Science and Engineering, Beijing University of Chemical Technology, Beijing 100029, China. E-mail: zhaobiao@mail.buct.edu.cn, dengjp@mail.buct.edu.cn*
[b]*School of Chemistry and Environmental Engineering, Yancheng Teachers University, Yancheng, 224007, China. E-mail: yuhl@yctu.edu.cn*

ductive to achieving high device efficiency. Among them, the study of chiral induced CP-PLEDs is based mainly on a system of small-molecule inducers. Compared with chiral small molecules, due to the unique chiral amplification effect, chiral helical polymers show higher-level chirality and stronger optical activity, providing an effective platform for constructing CPL materials with a high dissymmetry factor.

In view of the great achievements concerning CP-PLEDs in past years, a review article is very necessary at present, which is expected to activate and promote further progress in this unique research area. In this review, we systematically summarize recent progress in CP-PLEDs, in which the different types of polymer-based emitting materials are introduced in detail and highlighted. Additionally, the prospects and challenges for the future development of CP-PLEDs are also presented and discussed. We hope this review will stimulate further interest in polymer-based CPL materials and provide useful guidance for future research on CP-PLEDs with significant applications.

2. The basic concepts of CP-PLEDs

It is well known that OLEDs have gained extensive scientific and commercial attention due to their excellent brightness behaviour, high contrast, wide viewing angle, and fairly low power consumption, allowing them to be applied to panel displays and solid-state lighting. Similar to OLEDs, CP-PLEDs also have a typical sandwich device architecture, containing an anode, a hole transport layer (HTL), a chiral luminescent layer, an electron transport layer (ETL) and a cathode, as schematically illustrated in Fig. 1a. During operation, holes and electrons are first transfused into the ETL and HTL, respectively, and then recombined at the chiral luminescent layer to realize CPEL emission. By changing the emission wavelength of the chiral luminescent layer, multicolored CP-PLEDs can be obtained.

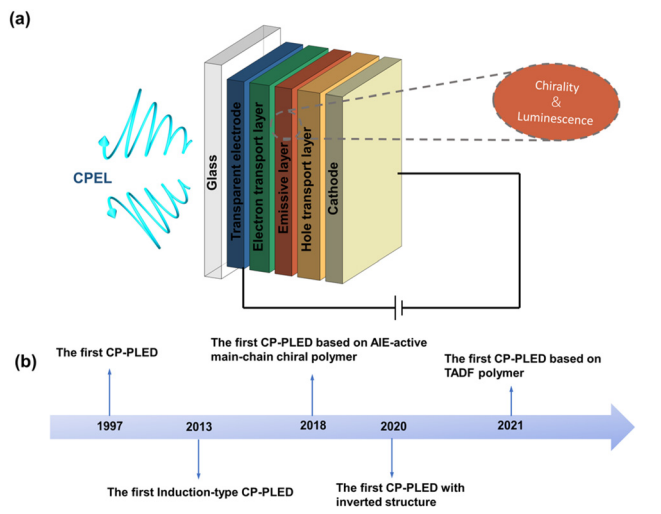

Fig. 1 (a) The basic device architecture of CP-PLEDs. (b) Timeline covering key achievements in the development of CP-PLEDs.

The first CP-PLEDs can be dated to 1997, but the development of CP-PLEDs has boomed in the past decade (Fig. 1b). The electroluminescence dissymmetry factor (g_{EL}) is an important index with which to evaluate the polarization performance of CP-PLEDs, and is defined as $g_{EL} = 2 \times (I_L - I_R)/(I_L + I_R)$, where I_L and I_R denote the left- and right-handed circularly polarized electroluminescence intensity, respectively. The range of g_{EL} is [−2, 2]. When $|g_{EL}| = 2$, it means complete CPEL emission, while $g_{EL} = 0$ means unpolarized electroluminescence. Apart from g_{EL}, device performance indexes, including luminance, turn-on voltage, EL spectra, luminescent efficiency, and lifetime are also critical parameters for CP-PLEDs. Achieving both a large g_{EL} value and high device performance is crucial for CP-PLEDs, which directly determines their practical application prospects.

3. CP-PLEDs based on chiral conjugated luminescent polymers

Generally, the coexistence of chirality and luminescence has been regarded as a necessary condition for CPL emission. By carefully bonding chiral and luminescent components into one entity, a series of CPL-active polymers for CP-PLEDs have been prepared. According to the relative position of the chiral unit, chiral luminescent polymers can be further classified into conjugated luminescent polymers with chiral side chains and conjugated luminescent polymers with chiral main chains, as well as the newly emerging CP-TADF polymers. The relevant studies are summarized in Table 1.

3.1. Conjugated luminescent polymers with chiral side chains

Bonding chiral side chains onto a conjugated luminescent polymer is an appealing strategy to create CPEL materials for CP-PLEDs. In 1997, Meijer and coworkers reported the first CP-PLEDs by using chiral π-conjugated poly(*p*-phenylenevinylene) (PPV) derivatives as an active layer.[17] As shown in Fig. 2a, a series of PPV derivatives, containing chiral BMB-PPV, chiral BMB-PPV-co-BDMO-PPV and racemic MDMO-PPV, were synthesized. Due to the absence of a chiral factor, no CPEL production was found in the polymer MDMO-PPV. In addition, although BMB-PPV could show CPL emission with a luminescence dissymmetry factor (g_{lum}) of -7.4×10^{-3}, the highly stereoregular and regiospecific substitution feature of the side chains favored aggregation, leading to low solubility in organic solvents and a failure to construct CP-PLEDs. Compared with the above two polymers, BMB-PPV-co-BDMO-PPV not only showed good solubility but also produced high chiroptical properties. The experimental results showed that BMB-PPV-co-BDMO-PPV exhibited a strong bisignate circular dichroism (CD) effect with an absorption asymmetry factor of -5.1×10^{-3} at 572 nm in film, accompanied by a CPL property with a g_{lum} value of -7.5×10^{-3} at 625 nm in solution. After using BMB-PPV-co-BDMO-PPV as an emitting layer (EML), CP-PLEDs

Table 1 Overview of reported CP-PLEDs based on chiral conjugated luminescent polymers

Category	Year	Structure	$\lvert g_{EL}\rvert_{max}$	L_{max}, cd m^{-2}	EQE_{max}, %	CE_{max}, cd A^{-1}	EL peak, nm	Ref.
Polymer with chiral side chains	1997	ITO/EML/PHWB601	1.7×10^{-3}	—	—	—	599	17
	2000	ITO/EML/Al	0.25	—	—	—	512	19
	2002	ITO/EML/Al	0.25	—	—	—	422	30
	2003	ITO/PEDOT:PSS/C-522/TPBi/LiF/Mg:Ag	0.35	—	—	0.94	-	31
	2017	ITO/Ca/TFP/c-PFBT/Ca/Ag	0.8	2950	—	—	545	20
	2019	ITO/PEDOT:PSS/P*/LiF/Al	0.2	—	—	—	425	32
Polymer with chiral main chains	2018	ITO/PEDOT:PSS/*S*-/*R*-P/TPBi/Ca/Ag	0.024	1669	—	0.926	512	34
	2022	ITO/PEDOT:PSS/26DCzPPy:chiral polymers/TPBi/Ca/Ag	1.0×10^{-3}	3013	0.54	0.81	460, 610	35
CP-TADF polymers	2019	ITO/PEDOT:PSS/EML/TmPyPB/LiF/Al	—	1477	10.3	2.52	529–571	26
	2021	ITO/PEDOT:PSS/mCP:pTpAcDPS/pTpAcBP/TmPyPB/LiF/Al	1.6×10^{-3}	6094/34 350	13.9/22.1	35.3/58.1	496/534	39
	2022	ITO/PEDOT:PSS/mCP:*R*-P/*S*-P/TPBi/LiF/Al	1.6×10^{-3}	12 180	15.8	54.0	546	40
	2023	ITO/PEDOT:PSS/*R*-P/TPBi/LiF/Al	1.7×10^{-3}	—	6.2	—	662	41
	2023	ITO/PEDOT:PSS/mCP:*R*-pSACODP/TPBi/LiF/Al	1.3×10^{-3}	9654	12.0	43.8	581	27
	2024	ITO/PEDOT:PSS/*R*-PBN or *S*-PBN/TmPyPB/LiF/Al	0.07	—	9.8	22.0	490	28
	2024	ITO/ZnO/PEIE/cPF8PhO8:(*R*)-BN-MDPA/CBP/TCTA/MoO_X/Au	0.091	100	0.18	0.52	553	48

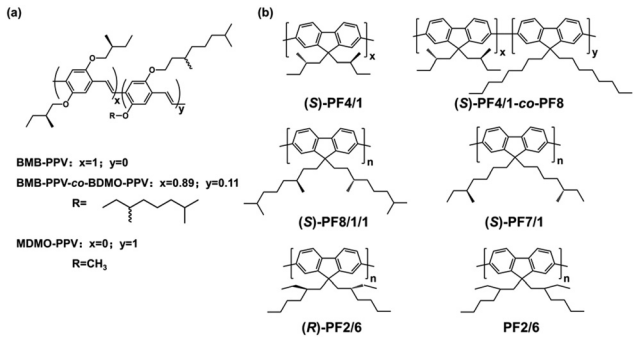

Fig. 2 (a) Chemical structures of BMB-PPV, BMB-PPV-co-BDMO-PPV and MDMO-PPV. Reproduced with permission.[17] Copyright 1997, American Chemical Society. (b) Chemical structures of chiral alkyl side chain substituted liquid crystal polyfluorene homopolymers. Reproduced with permission.[30] Copyright 2002, American Chemical Society.

with a maximum g_{EL} value of -1.7×10^{-3} centered at 600 nm were obtained. Moreover, the EL spectrum showed a similar profile to the PL spectrum of the thin film, demonstrating that the emission originated from the intrinsic luminescence of BMB-PPV-co-BDMO-PPV. This work has opened up a new field of direct CPEL emission based on OLED devices.

Polyfluorene (PF) derivatives are considered to be ideal electroluminescent materials because of their excellent carrier mobility and high orientation of thermotropic liquid crystal behaviour at high temperature.[29] In 2000, Neher and Scherf *et al.* showed the electroluminescence of CPEL with a large asymmetry factor using chiral substituted PF as an emission component. Chiral poly{2,7-[9,9-bis-(2*S*-2-methylbutyl)]-fluorene} and poly{2,7-[9,9-bis-(3*S*-3,7-dimethyloctyl)]-fluorene} were synthesized *via* Yamamoto-type polycondensation with Ni $(COD)_2$ as an effective aryl–aryl coupling agent.[19] Basing on the chiral amplification effect of liquid crystals, they also designed and reported a series of chiral alkyl side chain substituted liquid crystal PF homopolymers (Fig. 2b).[30] For the prepared polyfluorene derivatives, only after high-temperature annealing into the liquid crystal state can they exhibit significant chiral optical activity. A CP-PLED with a single-layer light-emitting diode structure was further prepared by using the homopolymer as the EML, and its g_{EL} value could reach 0.25.

Chen *et al.* also designed chiral conjugated PF oligomers to construct a CP-PLED (Fig. 3a).[31] Novel nonafluorenes with a varying extent of pendant chirality were synthesized for an investigation into the origins of chiroptical activities in neat films. These films had undergone thermal annealing treatment, which produced monodomain glassy films characterized as a right-handed cholesteric stack, and they exhibited obvious CD and CPL performances. Selecting C-522 for further device preparation, the blue-emitting CP-PLED exhibited an extremely high g_{EL} value of 0.35. However, the efficiency of the CP-PLED was low. At a current density of 20 mA cm^{-2}, this device exhibited a luminance yield of only 0.94 cd A^{-1}.

Apart from the intrinsic chiroptical activity of chiral luminescent materials, their thickness within an electroluminescent device may also play an important role in the final CPEL performance. In 2017, Nuzzo *et al.* prepared CP-PLEDs by taking a cholesteric poly(fluorene-*alt*-benzothiadiazole) (c-PFBT) with enantiomerically pure chiral side-chains as the emitting layer, and explored in detail the influence of the thickness of c-PFBT on CP-PLED performance (Fig. 3b).[20] The device structure of the CP-PLEDs is shown in Fig. 3b, in which indium tin oxide (ITO), poly(ethylenedioxythiophene):poly(styrenesulfonate):perfluorinated resin (PEDOT:PSS:PFI), poly[2,7-9,9-di-*n*-octylfluorene-*alt*-1,4-phenylene-4-sec-butylphenylimino-1,4-phenylene] (TFB), and Ca/Ag acted as anode, hole

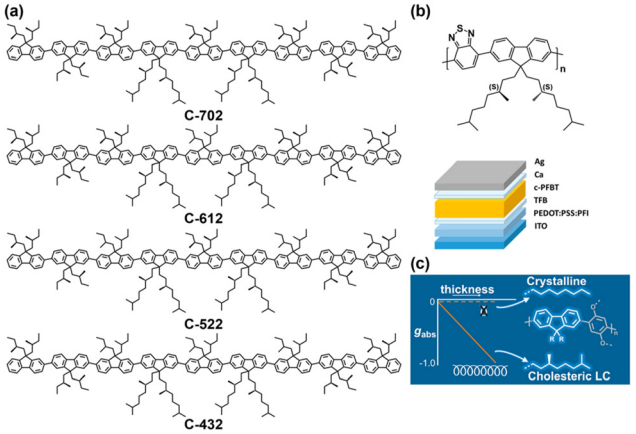

Fig. 3 (a) Chemical structures of chiral conjugated polyfluorene oligomers. Reproduced with permission.[31] Copyright 2003, American Chemical Society. (b) Chemical structures of donor–acceptor polyfluorene with chiral side chains, and the device structure of the CP-PLED. Reproduced with permission.[20] Copyright 2017, American Chemical Society. (c) Chemical structures of poly-(9,9′-dialkylfluorene-*alt*-2,5-dialkoxyphenyl), and the interaction diagram. Reproduced with permission.[32] Copyright 2019, American Chemical Society.

injection layer, electron blocker, and double-layered cathode, respectively. By adjusting the concentration of c-PFBT, the thickness of the c-PFBT layer was varied from 100, to 200 and 400 nm thickness. It was found that by increasing the thickness of the cPFBT layer, the g_{EL} value increased significantly, changing from −0.08 (100 nm thickness) to −0.6 (400 nm thickness), and could further increase to −0.8 under pulsed-voltage operation. Furthermore, Mueller matrix ellipsometry showed strong optical anisotropies in the film, which indicated that the circular polarization process occurred during the passage of photons through the thick film in the outward direction, through selective scattering and birefringence correlated in the direction of the initial linear polarization of the photon. This work offers a new insight into improving the g_{EL} values of CP-PLEDs by changing the thickness of the EML.

To understand the role of molecules with chiroptical properties in enantiomer π-conjugated polymers for organic light-emitting diode applications, in 2019, Meijer *et al.* studied a series of copolymers of poly-(9,9′-dialkylfluorene-*alt*-2,5-dialkoxyphenyl) with changes in the position and configuration of the chiral side chain in the repeating unit (Fig. 3c).[32] They found that the chiral side chains of the copolymers could produce extremely ordered cholesterol liquid crystals, which therefore show strong chiral absorption and photoluminescence properties in the annealed films, which are essential for the preparation and realization of CP-PLEDs with high g_{EL} values (>0.1).

3.2 Conjugated luminescent polymers with chiral main chains

Conjugated luminescent polymers with chiral main chains can also be used as CPEL materials for CP-PLEDs. To construct high-performance OLEDs, high-efficiency solid luminescent materials are also essential. However, traditional emitters usually suffer from a serious aggregation-caused quenching (ACQ) effect in aggregate and/or solid states, greatly limiting their practical application in OLEDs. Tang and coworkers were delighted to report aggregation-induced emission (AIE) luminogens in 2001,[33] which could emit remarkable fluorescence in aggregated states, introducing promising emitters for non-doped OLEDs. The rational combination of AIE unit and chiral unit into one entity may be an effective strategy to obtain CPL-active polymers for efficient CP-PLEDs. In 2018, Cheng, Quan and coworkers reported a pair of AIE-active chiral binaphthyl polymers (*S*-/*R*-P) through a Pd-catalyzed Suzuki coupling polymerization reaction.[34] The synthesized chiral polymer exhibited an obvious AIE property, showing high solid-state luminescence emission in the spin-coated film with a quantum yield of 14.8%. Besides, mirror-image CD bands and CPL signals were also observed in the film state, with g_{lum} values of 1.1×10^{-3} and -1.3×10^{-3}, respectively. Further, taking advantage of the AIE feature, doping-free green-colored CP-PLEDs with *S*-/*R*-P as the emitting layers were successfully prepared by a solution processing method, and the resulting devices displayed a turn-on voltage (V_{on}) and maximum brightness (L_{max}) of 6.0/5.7 V and 1669/1270 cd m^{-2}, respectively. Moreover, the device could emit strong CPEL signals with g_{EL} values of 2.4×10^{-2} and -1.9×10^{-2}, respectively.

It is well acknowledged that multicolored and white emissions are important in display technology, and the fabrication of full-color CPL materials as well as corresponding OLEDs is attracting intense interest. In 2022, Cheng and coworkers polymerized a functionalized bis-benzoxanethonyl unit as a rigid chiral source with three color groups to obtain three chiral polymers (*S*-/*R*-BP, *S*-/*R*-WP1, and *S*-/*R*-WP2), and constructed multicolored CP-PLED devices through solution treatment.[35] The three chiral functionalized bis-benzoxanethonyl polymers can emit different colors by adjusting the content of color groups, as shown in Fig. 4. Among them, *S*-/*R*-WP2 realized standard white CP-PLEDs with a high color rendering index of 95 and CIE coordinates of (0.33, 0.34) by an intramolecular chirality transfer mechanism from the chiral blue part to the achiral red dye through the polymer chain. Besides, the white CP-PLED showed a V_{on} of 5.8 V, a high L_{max} of 3000 cd m^{-2}, and a stable g_{EL} value of 10^{-3} in the wavelength range of 425–760 nm.

3.3 CP-TADF polymers

For traditional organic fluorescent materials, only 25% of singlet excitons can be utilized directly in OLEDs, leading to poor device efficiency with a theoretical EQE of only 5%. To address this issue, TADF molecules, regarded as third-generation luminescence materials for OLEDs, have been rapidly developed in the past decade. Purely organic TADF emitters can efficiently convert triplet excitons to singlet excitons through reverse intersystem crossing (RISC) due to the tiny energy gap (ΔE_{ST}) between the singlet and the triplet state, and then realize theoretical 100% internal quantum efficiency

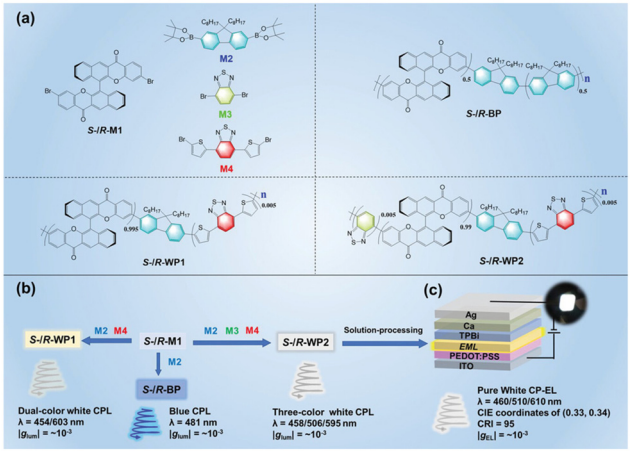

Fig. 4 (a) Chemical Structures of S-/R-M1, S-/R-BP, S-/R-WP1, and S-/R-WP2; (b) Schematic diagram of the route for blue and white CPL; (c) Device configuration of the CP-PLEDs. Reproduced with permission.[35] Copyright 2022, Wiley-VCH.

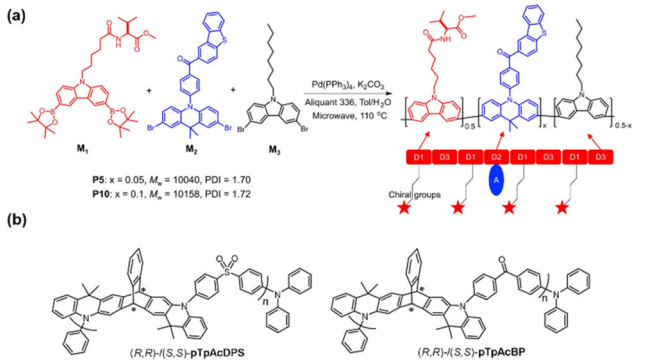

Fig. 5 (a) Synthetic route of chiral poly(carbazole-ran-acridine)s with TADF property. Reproduced with permission.[26] Copyright 2019, American Chemical Society. (b) Chemical structures of (*R*,*R*)-/(*S*,*S*)-pTpAcDPS and (*R*,*R*)-/(*S*,*S*)-pTpAcBP. Reproduced with permission.[39] Copyright 2021, Wiley-VCH.

(IQE). Therefore, TADF materials can serve as an ideal emissive layer to construct high-performance OLEDs. In the past few years, adopting intrinsic chirality and chiral perturbation strategies, scientists have designed and synthesized a series of small-molecule-based CP-TADF materials based on different chiral elements (including point chirality, axial chirality, facial chirality and helical chirality), and full-color CP-OLEDs have been constructed from them with a maximum EQE of over 30%.[36–38] However, at present, the g_{lum} factor of small-molecule-based CP-TADF devices is mostly below the order of 10^{-2}, which is far from meeting the needs of practical applications.

Compared with small-molecule-based CP-TADF materials, CP-TADF polymers show outstanding advantages in material selection, stability and device preparation, including: (1) CP-TADF polymers possess abundant chemically modifiable sites, and their emission color and carrier transport ability can be flexibly adjusted by regulating the structural unit; and (2) CP-TADFs show good morphological stability, thermal stability, machinability and excellent solubility, which provide the basis for the preparation of low-cost, solution-processable, large-area and flexible OLEDs. In 2019, Tang, Ma, Lam and coworkers reported the first CP-TADF polymer based on conjugated poly(carbazole-ran-acridine) with dibenzothiophen-2-yl (phenyl)methanone and a chiral alanine pendant *via* a Suzuki coupling reaction, as shown in Fig. 5a.[26] The synthesized polymer showed bright green photoluminescence emission in solid film with a quantum yield of 10.3%, and the delayed fluorescence lifetime was 1.366 μs. Moreover, a CPL property was also detected in the solid state with a g_{lum} value of -1.39×10^{-3}. The polymer solution was treated as an EML to prepare CP-PLED devices with L_{max} of 1477 cd m^{-2} and a current efficiency (CE) of 2.52 cd A^{-1}. Although the CPEL properties of the conjugated polymers were not detected, this work opens up a new perspective for designing highly efficient chiral emitters for use in CP-PLEDs.

Chen and coworkers made great efforts on CP-TADF polymer based CP-PLEDs.[39] In 2021, based on a chiral donor–acceptor copolymerization strategy, Chen, Li and colleagues synthesized two pairs of chiral nonconjugated main-chain polymers, (*R*,*R*)-/(*S*,*S*)-pTpAcDPS and (*R*,*R*)-/(*S*,*S*)-pTpAcBP, in which triptycene scaffold-based acridine (TpAc) was used as a chiral donor, while benzophenone diphenyl sulfone (DPS) and benzophenone (BP) were used as achiral receptors (Fig. 5b). Due to the unique alternating structure of donors and acceptors, the frontier molecular orbitals could be effectively separated, leading to prepared chiral polymers with strong TADF properties and a high PLQY of 92%. Besides, the introduction of a chiral donor enabled the resulting polymers to show intense chiroptical properties, exhibiting strong CPL activity with a g_{lum} value of 1.4×10^{-3}. Furthermore, by doping the prepared CP-TADF polymers in 1,3-bis(*N*-carbazolyl)benzene (mCP) as an emitting layer, solution-treated CP-PLEDs were constructed, with a maximum g_{EL} value of 1.6×10^{-3}, EQE_{max} of 22.1% and L_{max} value of 34 350 cd m^{-2}. Although the corresponding g_{EL} values of the CP-PLEDs were of the order of 10^{-3}, this work provides valuable guidance for the development of high-efficiency CPEL polymers.

In addition, using donor–acceptor copolymerization and chiral perturbation strategies, Chen and coworkers further synthesized a series of chiral TADF-active polymers with chiral groups located on the polymer main chain or side chain, and constructed CP-PLED devices with different emission colors.[27,40,41] To further improve the efficiency and g_{EL} factor, the authors recently prepared chiral conjugated TADF polymers named *R*-PAC and *S*-PAC by integrating an axially chiral biphenyl luminescent skeleton and benzophenone.[42] The introduction of the strong electron acceptor benzophenone could effectively separate the highest occupied molecular orbital (HOMO) and the lowest unoccupied molecular orbital (LUMO) of the chiral conjugated polymers, realizing a TADF feature with a small ΔEST of 0.05 eV. Besides, the obtained polymers exhibited a high PLQY of 82%, as well as strong CPL

emission with g_{lum} value of 3×10^{-3}. Solution-processed CP-PLEDs were further fabricated, showing a high g_{EL} value of 3.4×10^{-3} and EQE_{max} of 17.8%, which was the highest among the reported TADF-based CP-PLEDs at the time. The study demonstrates that the copolymerization of a chiral conjugated emitting skeleton and conjugated acceptor may be an effective strategy for achieving high-performance CP-PLEDs.

With the growing demand for a better visual experience, exploiting narrow-bandwidth-emission organic fluorescent materials for OLEDs with high color purity has attracted ever-increasing interest.[43] Since the first study on multiple resonance thermally activated delayed fluorescence (MR-TADF) molecules reported by Hatakeyama *et al.* in 2016,[44] synthesizing MR-TADF materials with a narrow full width at half maxima (FWHM) and high quantum yields has consistently fueled research interest in the realm of organic electronics,[45] which has also boosted the development of chiral MR-TADF molecules for CP-OLEDs.[46,47] Very recently, Chen, Li and co-workers reported a pair of self-assembled chiral MR-TADF polymers *R*-PBN/SPBN by introducing a chiral BN-moiety into a polyfluorene backbone through a Suzuki–Miyaura reaction, as shown in Fig. 6.[28] The resulting polymers showed narrow-band emission centered at 490 nm with an FWHM of 29 nm and a high PLQY of 79%. More importantly, due to the self-assembly feature, the chiral polymers could exhibit remarkable CPL emissions with g_{lum} up to 0.11 after thermal annealing treatment at 140 °C for ten minutes. Moreover, by taking the chiral polymers as CPEL, solution-processed non-doped CP-PLEDs with a maximum EQE of 9.8%, a large $|g_{EL}|$ of 0.07, and a small FWHM of 36 nm were further prepared. The work provides a promising method for fabricating advanced CP-PLEDs with both high color purity and high device efficiency.

Recently, in order to achieve high levels of CPEL produced by TADF materials, Fuchter, Colman and coworkers demonstrated a host–guest strategy for energy transfer between a chiral polyfluorene host (cPF8PhO8) and a novel chiral TADF-emitting material (*R*/*S*-BN-MDPA), which can result in the circular polarization of the emitter being effectively amplified.[48] After doping 10 wt% *R*/*S*-BN-MDPA into the cPF8PhO8 host through fluorescence resonance energy transfer (FRET), a CPEL signal with a g_{EL} value of 0.091 can be obtained by a CP-TADF emitter. This study provides further insights into the use of FRET in donor–acceptor materials as an effective strategy to achieve high levels of CP-TADF material development.

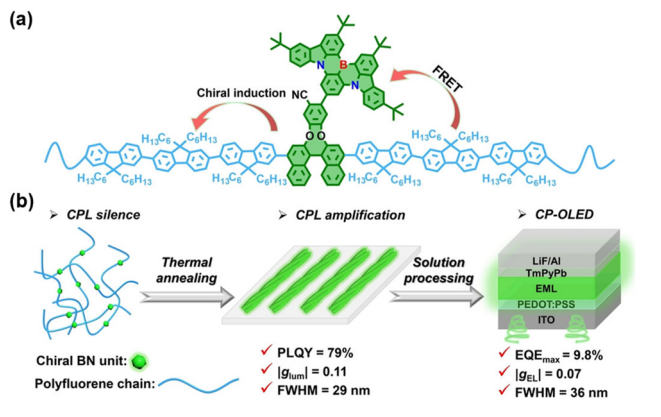

Fig. 6 (a) The design strategy of self-assembled chiral polymers *R*-PBN/SPBN. (b) A schematic diagram of chiral polymers with self-assembly behaviour in CP-PLEDs. Reproduced with permission.[28] Copyright 2024, Wiley-VCH.

4. CP-PLEDs based on achiral conjugated luminescent polymers doped with chiral inducers

Compared with CPEL emitter based chiral conjugated luminescent polymers, preparing CPEL emitters by doping chiral inducers in achiral conjugated luminescent polymers is more promising due to the simplified synthesis route and varying types of achiral emitters and chiral inducers, and has attracted increasing attention in recent years. In this method, selecting a suitable chiral inducer and establishing an efficient chiral transfer strategy are very important in successfully fabricating CP-PLEDs. Nowadays, various chiral inducers, including chiral small molecules (such as helicenes and binaphthol derivatives), chiral polymers as well as external environmental induction techniques, have been developed to prepare CP-PLEDs with high g_{EL} and good electrical properties. The relevant studies are summarized in Table 2.

4.1 Small-molecule-based chiral inducers

Recently, researchers have increasingly employed a method that involves mixing achiral polymers with chiral small-molecule additives in the active layer of OLEDs to generate CPELs. It is well known that helicenes are intrinsically helical and chiral conjugated molecules based on fused carbocyclic or heterocyclic rings. In 2013, Campbell, Fuchter and coworkers employed helicenes (1-aza[6]H, Fig. 7a) as chiral dopants to endow conventional achiral conjugated poly[(9,9-di-*n*-octylfluorenyl-2,7-diyl)-*alt*-(benzo[2,1,3]-thiadiazol-4,8-diyl)] (F8BT) with chirality. Additionally, they capitalized on the organic semiconducting characteristics of helicenes and polymers to ensure the effective operation of direct CP-PLED devices.[21] Following their experimental work, both enantiomeric devices exhibited bright emission with a measured luminance of 3000 cd m^{-2} and a PE of 1.1 lm W^{-1}. This research successfully demonstrated an effective approach to directly generate high levels of CPEL.

Generally, the chirality of the emitted CPEL is controlled by the absolute stereochemistry of chiral small molecules. However, Campbell and Fuchter *et al.* reported that by combining chiral 1-aza[6]H and achiral F8BT, it was possible to emit left-handed (LH) or right-handed (RH) CPEL, depending on the thickness of the active layer, as shown in Fig. 7b.[22] Besides, efficient and bright CP-PLEDs with a CE up to 4.0 cd A^{-1} and an L_{max} value of 8000 cd m^{-2} could be achieved. The

Table 2 Overview of the reported CP-PLED based on achiral conjugated luminescent polymers doped with chiral inducers

Category	Year	Structure	$\lvert g_{EL}\rvert_{max}$	L_{max}, cd m^{-2}	EQE_{max}, %	CE_{max}, cd A^{-1}	EL peak, nm	Ref.
Small-molecule-based chiral inducers	2020	ITO/PEDOT:PSS/F8BT:*R*/*S*-3/TPBi/Ca/Ag	5.9×10^{-3}	14 661	2.17	2.51	460	54
	2021	ITO/PEDOT:PSS/F8BT:*R*/*S*-6/TPBi/Ca/Ag	8.42×10^{-3}	16 730	1.02	3.23	545	55
	2017	ITO/CuPc/Polymide/F8BT:S5011/TPBi/LiF/Al	1.13	—	—	—	546	56
	2018	ITO/CuPc/Al22636/F8BT:S5011/TPBi/Al	0.79	—	—	—	546	57
	2024	ITO/PEDOT:PSS+PFI/(F8BT)0.9-(*R*/*S*-5011) 0.1-(DBN-ICZ)0.005/TPBi/LiF/Al	0.16	25 000	4.3	17.7	552	58
	2013	ITO/PEDOT:PSS/F8BT:1-aza[6]H/Ca/Al	0.2	3000	—	—	546	21
	2019	ITO/PEDOT:PSS/TFB/F8BT:1-aza[6]H/Ca/Al	1.10	8000	—	4.0	545	22
	2020	ITO/ZnO/PEIE/F8BT:1-aza[6]H/MoO_x/Au	0.57	28 500	—	16.4	545	49
	2021	ITO/ZnO/PEIE/TPBi/PFO:1-aza[6]H/TCTA/MoO_x/Au	0.44	1583	—	1.23	434	51
	2022	ITO/PEDOT:PSS/TFB/F8BT:1-aza[6]H:EDA/Ca/Al	0.65	—	—	—	525/580	50
	2022	ITO/PEDOT:PSS/TFB/FBT2:1-aza[6]H/Ca/Al	0.3	3023	—	0.53	546	53
	2022	ITO/PEDOT:PSS/PVK/PFO:*S*-F4SO/CsF/Al	4.5×10^{-3}	6440	—	1.8	448	52
	2023	ITO/PEDOT:PSS/(BP/*w*-WP/*c*-WP)/TPBi/Ca/Ag	0.062	9344	1.45	3.04	450/516/604	59
	2023	ITO/PEDOT:PSS/$(S$-/R-2Cz$)_{0.2}$(PFpy$)_{0.8}$-(Ir(MDQ)$_2)_{0.1}$/TPBi/Ca/Ag	0.014	21 019	4.1	7.0	620	60
Polymer-based chiral inducers	2021	ITO/PEDOT:PSS/Bpy:*R*/*S*-P2/TPBi/Ca/Ag	0.021	205	—	0.38	420	61
	2022	ITO/PEDOT:PSS/$(R/S$-P2$)_{0.6}$-(NPy$)_{0.4}$/TPBi/Ca/Ag	0.048	3018	0.21	1.72	489	63
	2023	ITO/ZnO:Mg/F8BT:P37/TCTA/MoO_3/Al	0.02	35 303	1.20	3.67	546	23
External environment	2019	ITO/CuPc/PI/F8BT/TPBi/LiF/Al	0.64	—	—	1.0	550	64
	2020	ITO/PEDOT:PSS/F6BT/TPBi/LiF/Al	4.16×10^{-3}	1893	0.11	0.32	554	65

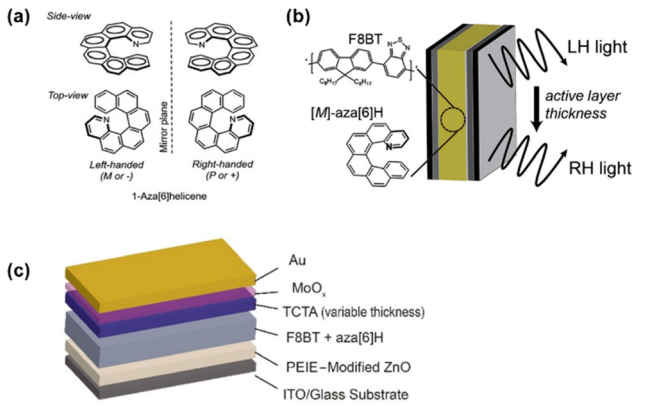

Fig. 7 (a) Chemical structures of 1-aza[6]H. Reproduced with permission.[21] Copyright 2013, Wiley-VCH. (b) Schematic diagram illustrating the adjustment of CP light by 1-aza[6]H as a function of active layer thickness. Reproduced with permission.[22] Copyright 2019, American Chemical Society. (c) Inverted device architecture. Reproduced with permission.[49] Copyright 2020, American Chemical Society.

CP-OLED device emitted strong CPEL emission, and when the EML thickness was 110 nm and 160 nm, the g_{EL} values were 0.51 and −1.05, respectively. This study provides profound insights into the mechanism of CPEL generation in CP-PLEDs and demonstrates new opportunities for the design of CP photonic devices.

In 2020, to solve the problem of CP-PLEDs suffering from low g_{EL} and poor device performance, Campbell and Fuchter *et al.* demonstrated the first CP-PLEDs employing an inverted device architecture, as shown in Fig. 7c.[49] The resulting CP-PLEDs demonstrated a CE of 16.4 cd A^{-1}, a power efficiency of 16.6 lm W^{-1}, an L_{max} of up to 28 500 cd m^{-2}, and a high g_{EL} of 0.57. Moreover, they found that the handedness of the emitted light was sensitive to the device architecture. In detail, the sign of CPEL from an identically prepared active layer reversed between inverted and conventional devices. These findings significantly broaden the versatility of CP emissive devices and should enable their further application in a variety of CP-dependent technologies. To solve the unbalanced charge transport and unfavorable energetics between chiral additives 1-aza[6]H and achiral conjugated polymers F8BT, which would limit the efficiency of charge injection and device performance, Kwon, Fuchter, Kim and colleagues also proposed the use of a small amount of chemically modified electrochemical doping agent (EDA) to overcome this limitation.[50] After adding EDA components, a uniform ternary blend system was formed, and the resulting CP-PLED exhibited efficient carrier injection and balance and maintained a high $|g_{EL}|$ of up to 0.5 at 580 nm.

Poly(9,9-dioctylfluorene) (PFO) has been developed as the main material for deep-blue polymer light-emitting diodes due to its excellent solution processing properties, wide bandgap and high photoluminescence quantum efficiency. In 2021, Campbell, Fuchter and collaborators mixed PFO with 1-aza[6]H and prepared CP-PLEDs devices through solution treatment, achieving blue CPL emission with high device performance.[51] They used an inverted device with a planarized and extended "β phase" structure with a CE of 1.23 cd A^{-1}, PE of 0.63 lm W^{-1}, and g_{EL} of −0.44. Compared with the semi-crystalline phase, the embedding of the β phase improved the device efficiency, efficiency roll-down and g_{EL}, and can provide

further insight into the mechanism of the high chiral optical activity of polyfluorene materials. In 2022, Zhong, Peng, and Guo *et al.* introduced a left-handed blue-light-emitting molecule called S-F4SO. This molecule was designed with a dibenzothiophene-*S*,*S*-dioxide (SO) core and bi-fluorene arms. Interestingly, S-F4SO exhibited weak CD and CPPL signals.[52] When S-F4SO was blended with PFO, the CD and CPPL signals could be enhanced dramatically. Moreover, when the mixing ratio of PFO : S-F4SO was 7 : 3 wt%, the strongest CD and CPPL signals could be obtained, and the corresponding CPEL also showed a g_{EL} of 4.5×10^{-3} with maximal emission at 448 nm. Furthermore, the blends demonstrated a CE_{max} of 1.8 cd A^{-1} with CIE coordinates of (0.16, 0.10) as well as excellent EL stability.

Apart from the above achiral polyfluorene derivative, poly (9,9-dioctylfluorene-*alt*-bithiophene) (F8T2) is also a typical semiconductor polymer, which has been widely used as an active layer in optoelectronic devices. In 2022, Fuchter and co-workers reported CP-PLEDs using a blend of F8T2 and a chiral small-molecule additive (1-aza[6]H).[53] The CP-PLEDs exhibited a large g_{EL} factor over 0.3 and a CE of 0.53 cd A^{-1} and brightness of 3023 cd m^{-2}, as shown in Fig. 8. At low loadings of aza [6]H, F8T2 blends exhibited behavior consistent with previous observations, showing circularly polarized dissymmetry inversion in relation to film thickness and excitation mode. However, at higher loadings of 1-aza[6]H (approximately 40 wt%), these dependencies were eliminated while maintaining excellent g_{EL} factors.

Quan and Cheng *et al.* synthesized blue-emitting chiral enantiomers with a pyrene-containing group as a fluorophore and a binaphthalene derivative as a chiral source, and doped them with F8BT to construct solution-processed CP-PLEDs with excellent properties.[54] On that basis, they also designed and synthesized nine chiral binaphthyl derivatives (*R*/*S*-1–*R*/*S*-9, Fig. 9a) as CPEL inducers.[55] The molecular conformations and CPL behaviors of these chiral inducers were found to be significantly influenced by the length of the alkyl chain and the degree of substituent steric hindrance. These factors could further regulate their chiral induction effect on achiral fluorescent polymer F8BT in the doped films, ranging from small to large. Among them, *R*/*S*-1, *R*/*S*-6, and *R*/*S*-9 exhibited a planar and rigid conjugated molecular conformation, which resulted in a CPL signal with a high $|g_{PL}|$ value of 2.36×10^{-2} upon chiral induction of F8BT. A CP-PLED device based on blends of F8BT and R/S-6 with small dihedron angle and excellent carrier mobility showed a low V_{on} (<4.5 V), high brightness (>10 509.6 cd m^{-2}), and $|g_{EL}|$ value of 1.86×10^{-2}, as shown in Fig. 9b.

Additionally, Kim and Yu *et al.* detected an extremely high degree of CPPL and CPEL in an achiral conjugated polymer induced by a non-emitting chiral dopant (S5011). This effect was achieved through the twisted stacking of the polymer chains, and it marked the first instance of such high helical twisting power resulting in $|g_{PL}|$ = 0.72 and $|g_{EL}|$ = 1.13.[56] Through theoretical analysis incorporating the Stokes parameter, it was found that the key features for obtaining a high g

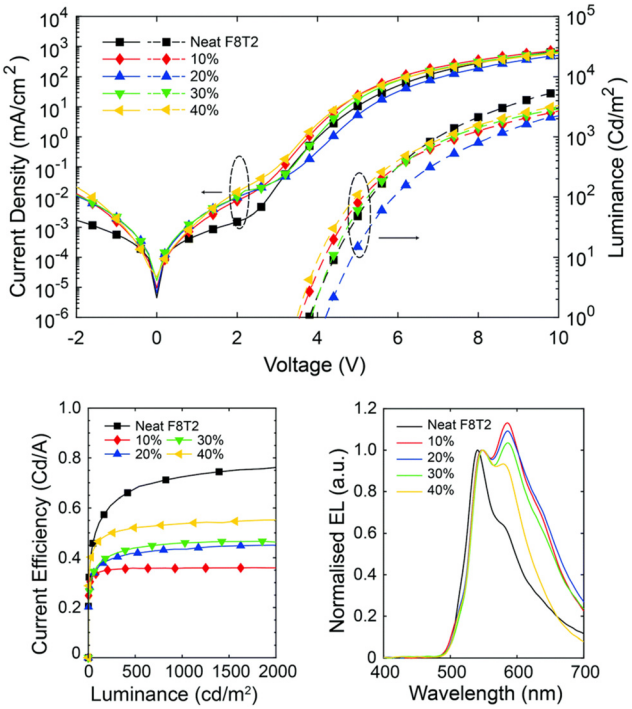

Fig. 8 *J*–*V*–*L*, CE and PE spectra of F8T2:aza[6]H devices with increasing active layer thickness. Reproduced with permission.[53] Copyright 2022, Royal Society of Chemistry.

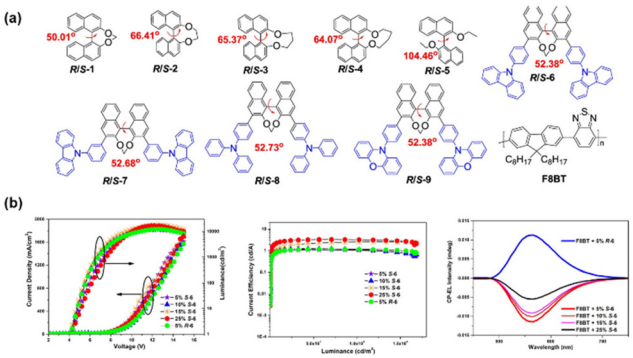

Fig. 9 (a) Chemical structures of *R*/*S*-1–*R*/*S*-9 and F8BT. (b) *J*–*V*–*L*, CE and CPEL spectra of devices based on blends of F8BT with various amounts of *R*/*S*-6. Reproduced with permission.[54] Copyright 2021, American Chemical Society.

value were the retardation and twist angle of the EML, and the degree of linear polarization of the emitted light. Moreover, they showed that the location of the recombination region within the EML was a key parameter in determining the difference in the dissymmetry factor between CPPL and CPEL.[57] This work contributes to the design of device structures that produce almost pure CP light, thus vastly improving their luminous efficiency.

Recently, Chen and Li *et al.* proposed a ternary chiral co-assembler that achieved narrowband multi-resonance characteristics by co-doped thermal annealing of the achiral lumines-

cent polymer F8BT, the chiral inducers *R*/*S*-5011, and the achiral FRET receptor DBN-ICZ.[58] The CP-PLED was prepared using $(F8BT)_{0.9}$-$(R/S\text{-}5011)_{0.1}$-$(DBN\text{-}ICZ)_{0.005}$ as the EML, which showed a yellow CPEL with EQE = 4.6% and a g_{EL} value of 0.16. In addition, these devices exhibited a low V_{on} value of 7.0 V, a high L_{max} value of 25 000 cd m^{-2} and narrowband EL with FWHM of only 39 nm. The ternary co-assembly strategy proposed in this study provides the possibility for achieving high integrated device performance.

To date, most CP-PLEDs based on chiral assembly EML have exhibited monochromatic emission. White circularly polarized organic light-emitting diodes (CP-WOLEDs), which directly emit circularly polarized light, have generated growing interest with potential applications in lighting and full-color 3D displays. In 2023, Quan and Cheng *et al.* employed three achiral conjugated pyrene-based dyes (BP, w-WP and c-WP) doped with chiral enantiomers (*S*/*R*-M) as EML to fabricate a full-color CPEL device.[59] This EML was constructed through a chiral co-assembly process facilitated by an intermolecular chiral induction mechanism, as shown in Fig. 10. After annealing, the $(S/R\text{-}M)_{0.2}$-$(c\text{-}WP)_{0.8}$ film presented regular helical nanofibers and emitted strong white CPL. By using the chiral co-assembled $(S/R\text{-}M)_{0.2}$-$(c\text{-}WP)_{0.8}$ as an EML for CP-PLED, the white-light CPEL exhibited a significant g_{EL} value of 6.2×10^{-2} and a color rendering index (CRI) of 98 at room temperature. Moreover, ideal white-color CIE coordinates of (0.33, 0.33) were achieved. This result of white CP-PLEDs based on chiral co-assembled helical nanofiber emitters provides a valuable strategy for developing a white CPEL with practical applications.

In 2023, Zhang *et al.* introduced a promising approach involving the utilization of a chiral co-assembled host derived from an achiral conjugated polymer acceptor doped with a chiral donor, alongside an achiral phosphorescent emitter employed as an EML for CP-OLEDs.[60] They synthesized a chiral co-assembled helix nanofiber material ($(R/S\text{-}2Cz)_{0.2}$-$(PFpy)_{0.8}$) through the interaction between the achiral conjugated pyridine-based polymer (PFpy) and the chiral binaphthyl-based molecule, as shown in Fig. 11a. The researchers found that when using $(R/S\text{-}2Cz)_{0.2}$-$(PFpy)_{0.8}$ as the chiral co-assembled main material of the phosphorescent emitter $Ir(MDQ)_2$ (Fig. 11b), they were able to achieve CP-OLEDs emitting red light at 620 nm, with an EQE up to 4.1% and a g_{EL} value of 0.014.

4.2 Polymer-based chiral inducers

The type of chiral inducer is critical to the final performance of CP-PLEDs. Until now, research on CP-PLEDs has been based mainly on small-molecule inducer systems. Compared with chiral small molecules, chiral polymers exhibit a higher level of chirality and strong optical activity due to their unique chiral amplification effect, and they provide an effective platform for constructing CPL materials with high asymmetric factors. In 2021, Cheng and colleagues proposed a new strategy to construct CP-PLEDs by using helical co-assemblies composed of chiral polymers and an achiral fluorophore (Bpy) as active layers.[61] They synthesized three chiral 1,1′-binaphthyl-based polymers (*R*/*S*-P1, *R*/*S*-P2 and *R*/*S*-P3) with different side chain alkyl groups (n-C_4H_9; n-C_6H_{13}; n-C_8H_{17}), as shown in Fig. 12a. Specifically, the *R*/*S*-P2 inducer doped with Bpy demonstrated the formation of helical nanofibers and emitted a robust deep-blue CPL signal at 420 nm. Moreover, a CP-PLED prepared by using *R*/*S*-P2-Bpy as an EML can exhibit an obvious CPEL signal. The structure, electrical properties, EL spectra and CPEL curves of the doped CP-PLEDs are shown in Fig. 12b.

It is well known that axial chiral binaphthyl derivatives can not only exhibit highly rigid plane conformation according to the anchoring dihedral angle of their binaphthyl groups, but they also greatly promote the amplification effect of their intrinsic molecular chirality and chirality induction ability.[62] In 2022, Quan, Cheng and coworkers used two chiral polymers, *R*/*S*-P1 and *R*/*S*-P2, with different binaphthyl dihedral

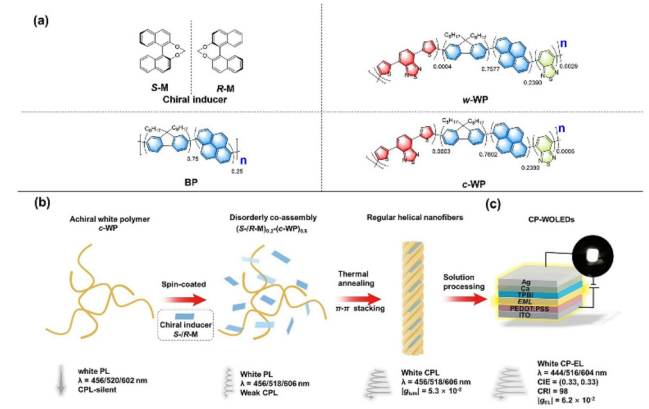

Fig. 10 (a) Chemical structures of *S*/*R*-M, BP, *w*-WP and *c*-WP. (b) Schematic diagram of the route to a white CPL. (c) Device structure of the CP-WOLEDs. Reproduced with permission.[59] Copyright 2023, Wiley-VCH.

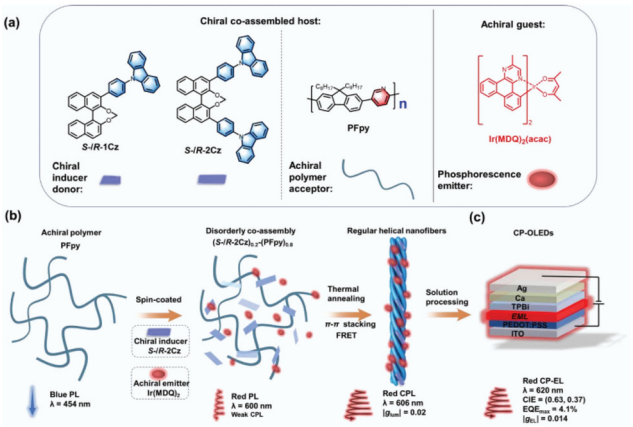

Fig. 11 (a) Chemical structures of *S*/*R*-1Cz, *S*/*R*-2Cz, PFpy, and Ir $(MDQ)_2$. (b) Schematic diagram of the route to a red CPL. (c) The device structure of the CP-OLEDs. Reproduced with permission.[60] Copyright 2023, Wiley-VCH.

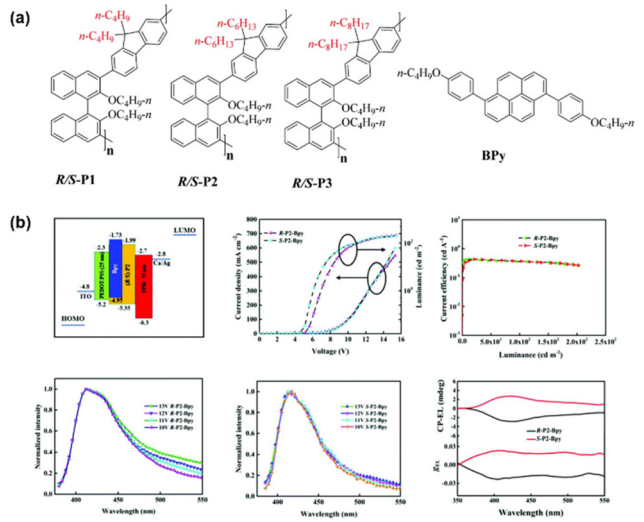

Fig. 12 (a) Chemical structures of *R*/*S*-P1, *R*/*S*-P2, *R*/*S*-P3 and BPy. (b) The device structure of the CP-PLEDs, and *J*–*V*–*L*, CE, EL spectra of the *R*-P2-Bpy device, EL spectra of the *S*-P2-Bpy device and the CPEL curves. Reproduced with permission.[61] Copyright 2021, Royal Society of Chemistry.

angles, as chiral inducers in combination with achiral pyrene-naphthalimide dyes (NPy) to construct chiral co-assemblies, as shown in Fig. 13.[63] The anchored dihedral angle of *R*/*S*-P2 showed a stronger chiral signal when combined with achiral NPy dye in the co-assembled $(R/S\text{-P2})_{0.6}$-$(\text{NPy})_{0.4}$, resulting in a stronger chiral induction effect. This specific combination formed a helical co-assembly structure through robust π–π packing interaction between *R*/*S*-P2 and the achiral NPy, facilitated by the adjustment of the rigid polymer R/S-P2 during chiral co-assembly. The ordered helical nanofiber $(R/S\text{-P2})_{0.6}$-$(\text{NPy})_{0.4}$, when annealed at 120 °C as an EML for CP-PLEDs, produced CPEL properties at 489 nm with $|g_{EL}|$ of 4.8×10^{-2}. This work provides a new idea for developing useful CP-PLEDs.

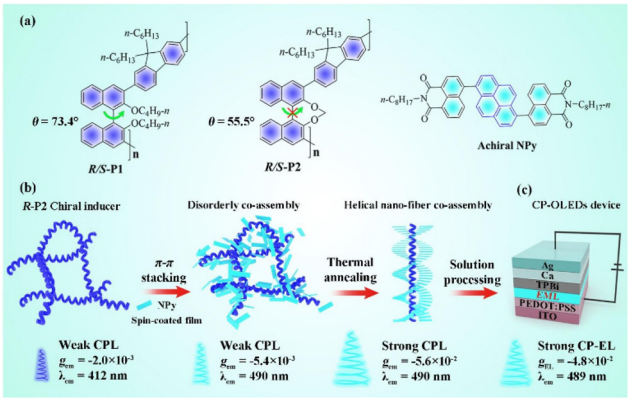

Fig. 13 (a) Chemical structures of *R*/*S*-P1, *R*/*S*-P2 and NPy. (b) Schematic diagram of the possible co-assembly route for $(R\text{-P2})_{0.6}$-$(\text{NPy})_{0.4}$. (c) Device structure of the CP-PLEDs. Reproduced with permission.[63] Copyright 2022, Wiley-VCH.

Chiral helical polymers can be also used as dopants to prepare CP-PLEDs with large g_{EL} values and high efficiency. In 2023, Deng and Zhao *et al.* utilized the helical substituted polyacetylene P37 as a chiral inducer, which was combined with conjugated polymer F8BT to construct efficient CP-PLEDs (Fig. 14).[23] The high helical twisting ability of P37 and the thermotropic liquid crystal properties of polyfluorene enabled the prepared CP-PLED to exhibited high g_{EL} values of up to 2.0×10^{-2}. In addition, when F8BT was induced by another chiral helical polymer PSA, the resulting CP-PLED also exhibited significant CPEL characteristics, confirming the universality of this strategy. Inverting the device structure notably enhanced the device performance, yielding an L_{max} of 49 340/51 973 cd m^{-2} and a CE of 5.62/5.44 cd A^{-1}. These findings provide valuable insights into the fabrication of CP-PLEDs by taking advantage of chiral helical polymers.

4.3 CPEL induced by external environment

Conventional strategies to directly generate CPEL from the EML of OLEDs, including the attachment of chiral pendants and the use of chiral additives, have been well developed. In 2019, Kim and Yu *et al.* introduced the concept of direct CPL emissions using a twisted achiral conjugate polymer F8BT without any chiral dopant in the EML.[64] The twisted structure is formed by applying different alignment directions to the upper and lower interfaces of the mesogenic conjugated polymer, as shown in Fig. 15a. For domains that twisted with left- and right-handedness in a single device, the high g_{PL} of the PL process were observed to be 0.60 and −0.63, respectively, showing opposite signs. Similarly, the g_{EL} of the EL process were observed to be 0.57 and −0.64, respectively.

In 2020, Qiu, Zou and coworkers showed that CP-PLEDs based on achiral poly(9,9-di-*n*-hexylfluorene-*alt*-benzothiadiazole) (F6BT) could be induced to emit preferentially left- or right-handed CPEL simply by treating them with CP light, as shown in Fig. 15b.[65] In this study, the initially achiral F6BT can be transformed into a predicted chiral helical conformation under irradiation by CP light, with a detailed exploration of the effects of chirality and wavelength of the driving CP

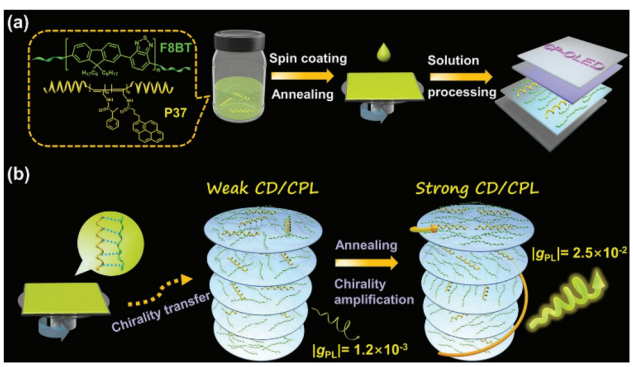

Fig. 14 (a) Chemical structures of F8BT and P37. (b) The mechanism of F8BT induced by P37. Reproduced with permission.[23] Copyright 2024, Wiley-VCH.

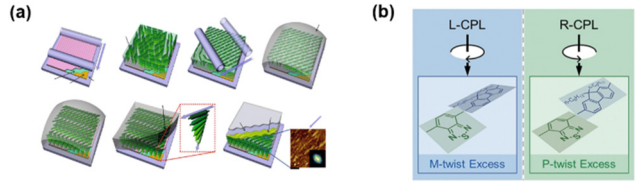

Fig. 15 (a) Schematic diagrams of the fabrication process. Reproduced with permission.[64] Copyright 2019, Springer Nature (b) scheme depicting the chirality induction of F6BT by left-(L-CPL) and right-handed circularly polarized light (R-CPL), respectively. Reproduced with permission.[65] Copyright 2020, Royal Society of Chemistry.

light. The induced device exhibited an obvious CPEL signal, with a $|g_{EL}|$ value of 4.16×10^{-3} at 554 nm. While the electrical properties of the resulting CP-OLED devices were not superior, this work offers a new insight into constructing low-cost CP-PLEDs.

5. CP-PLEDs based on chiral metal complexes

Due to their multiple coordination modes and rich excited states, transition metal complexes have been widely used to combine with organic molecules to prepare luminescent materials with fascinating luminescence properties. Based on the metal-to-ligand charge transfer effect, the metal complexes can also simultaneously harvest the energy of singlet and triplet states for light emission, thus theoretically increasing the IQE to 100%, which may be an ideal material system for constructing OLED devices with high luminous efficiency.

In 2021, You, Kim and coworkers developed a series of (*P*)-helical-sense-enriched polymer hosts and chiral Pt dopants for CP-PLEDs.[24] The polymer hosts were synthesized by the free-radical copolymerization of an achiral 3-vinylcarbazole monomer and a chiral 3-vinylcarbazole monomer with an (*R*)-α-phenylisopropyl moiety. The authors explored the diastereomeric interactions between the chiral polymer hosts and the phosphorescent chiral Pt dopants (Fig. 16a), and found that the chiroptical behaviors of the Pt(II) dopants are obviously affected by the local chiral environments provided by the polymer hosts. In detail, the Kuhn dissymmetry factor (g_{abs}) of an (*R*)-dopant/chiral polymer host was 5.7×10^{-4} at 391 nm, nearly 10-fold larger than that of an (*S*)-dopant/chiral polymer host, which was only 0.5×10^{-4} at 391 nm. Additionally, the doping films could show CPL emissions at around 540 nm with a g_{lum} value of the order of 10^{-3}. CP-PLEDs were further prepared using chiral doping films with 30% Pt dopant, showing g_{EL} values of 1.09×10^{-4} and -1.02×10^{-4} at 540 nm, together with an EQE of 1.2%.

In recent years, chiral Mn(II) complexes displaying CPL have attracted great interest due to their environmental friendliness, low cost, and room-temperature phosphorescence. In 2023, Lin, Meng and Artem'ev *et al.* reported the assembly of an Mn

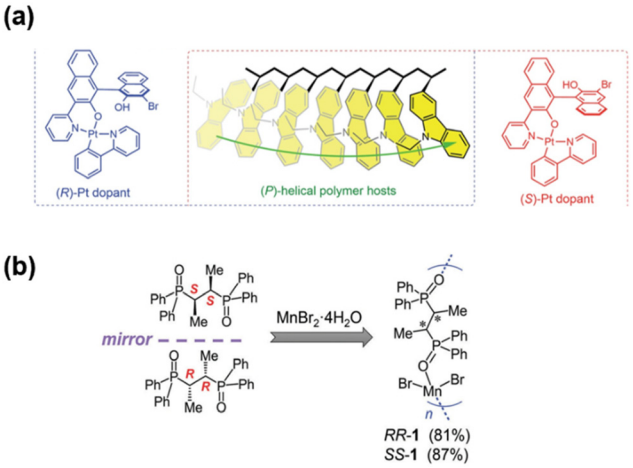

Fig. 16 (a) Chemical structures of (*R*/*S*)-Pt dopant. Reproduced with permission.[24] Copyright 2021, Royal Society of Chemistry. (b) Chemical structure of chiral Mn(II)-organic helical polymer. Reproduced with permission.[25] Copyright 2023, Wiley-VCH.

(II)-organic chiral helical polymer by bridging the $MnBr_2$ unit with chiral O,O'-linker ligands (Fig. 16b).[25] The resulting chiral Mn(II)-organic helical polymers displayed long-lived circularly polarized phosphorescence with a high g_{lum} of 0.021 and QY of 89%. In addition, the authors manufactured UV-pumped CPL light-emitting diodes that demonstrated enhanced optical selectivity under left- and right-handed polarization conditions. This work provides new insights into understanding the CPL phenomena in multi-spin compounds, which will contribute to the future development of Mn(II)-based CPL emitters with significant potential.

6. Conclusions and perspectives

This review provides a comprehensive summary of recent research advances in CP-PLEDs using a polymer-based chiral luminescent material as the active layer. By categorizing the reported chiral polymers, the construction strategies of these emitters can be mainly divided into chiral conjugated luminescent polymers, achiral conjugated luminescent polymers doped with chiral inducers, and chiral polymer-based metal complexes. It was found that researchers developed various polymers with CPEL activity, but few polymers can achieve both high g_{EL} and excellent electrical performance in the preparation of light-emitting devices. The main reason is that the selection of chiral materials is limited, and chiral molecules that produce CPL usually have low charge mobility, which affects the current density and carrier transport efficiency, thereby reducing the EL efficiency. Second, the generation of CPL depends on a specific molecular arrangement, but this structure may cause the molecular accumulation of the luminous material to be uneven, affecting the EL efficiency. In addition, the long-term stability of chiral

materials is poor, and they are easily degenerated under the driving current, shortening the life of the device. In order to solve these problems, molecular structures with high mobility and chirality should be designed in terms of materials. In the structure of the device, the interface modification layer is added to optimize the charge transfer to enhance the EL efficiency. Technically, the arrangement and stability of the material are improved by molecular orientation and a low-temperature process. Hence, the polarization efficiency and electrical performance of CP-PLEDs are further improved. So far, TADF polymers often demonstrate excellent photophysical properties and could be promising materials for preparing metal-free, CP-PLEDs with highly efficient device performance.

Although researchers have made significant progress in developing polymeric materials with CPEL properties and constructing corresponding CP-PLEDs, there are still numerous challenging obstacles in this field: (1) polymer-based chiral luminescent materials face difficulties in synthesis, complex routes, and poor induction effects, which still hinder the construction of efficient CP-PLEDs. (2) The preparation of both high g_{EL} and high-performance CP-PLEDs remains a major challenge that needs to be addressed and resolved in this field. (3) The detailed CPEL generation mechanism, especially the relationship between the device structure and CPEL performance (including magnitude and direction), is still unclear and needs to be investigated further. In conclusion, challenges and opportunities exist, and exploring various CPEL materials to construct efficient CP-PLEDs should still be the direction in which we apply our efforts. For example, a CP-PLED with a nonreciprocal CPEL property can achieve stronger polarization efficiency than conventional CP emitters. It avoids the phenomenon in which the polarization efficiency of the device is greatly reduced because the back-emitted light of the conventional emitter is partially reflected by the metal cathode, so that the total polarization output of the device can be increased. In addition, narrow-bandwidth emissive CP-PLEDs, and flexible and stretchable CP-PLEDs also have more diverse performance advantages, which are worth exploring. With the increasing attention paid to novel CPL-active polymers, we firmly believe that the above challenges can be solved in the near future and the progress of CP-PLEDs will undoubtedly be enhanced.

Data availability

No new data were generated or analyzed in this review. All the primary data supporting this review are available within the articles cited in the manuscript.

Conflicts of interest

There are no conflicts to declare.

Acknowledgements

This work was financially supported by the National Natural Science Foundation of China (52003022, 51973011 and 52273165), and the Fundamental Research Funds for the Central Universities (buctrc202225).

References

1 K. J. Voss and Y. Liu, *Appl. Opt.*, 1997, **36**, 6083–6094.
2 J. R. Brandt, X. Wang, Y. Yang, A. J. Campbell and M. J. Fuchter, *J. Am. Chem. Soc.*, 2016, **138**, 9743–9746.
3 S.-Q. Zhao, G. Hu, X.-H. Xu, S.-M. Kang, N. Liu and Z.-Q. Wu, *ACS Macro Lett.*, 2018, **7**, 1073–1079.
4 Y. Zhang, S. Yu, B. Han, Y. Zhou, X. Zhang, X. Gao and Z. Tang, *Matter*, 2022, **5**, 837–875.
5 Y. Sang, J. Han, T. Zhao, P. Duan and M. Liu, *Adv. Mater.*, 2020, **32**, 1900110.
6 B. Zhao, K. Pan and J. Deng, *Macromolecules*, 2018, **51**, 7104–7111.
7 B. Zhao, K. Pan and J. Deng, *Macromolecules*, 2019, **52**, 376–384.
8 H. Zhong, X. Gao, B. Zhao and J. Deng, *Acc. Chem. Res.*, 2024, **57**, 1188–1201.
9 H. Zhong, B. Zhao and J. Deng, *Adv. Opt. Mater.*, 2023, **11**, 2202787.
10 C. W. Tang and S. A. VanSlyke, *Appl. Phys. Lett.*, 1987, **51**, 913–915.
11 F. Song, Z. Xu, Q. Zhang, Z. Zhao, H. Zhang, W. Zhao, Z. Qiu, C. Qi, H. Zhang, H. H. Y. Sung, I. D. Williams, J. W. Y. Lam, Z. Zhao, A. Qin, D. Ma and B. Z. Tang, *Adv. Funct. Mater.*, 2018, **28**, 1800051.
12 M. Zhang, Q. Guo, Z. Li, Y. Zhou, S. Zhao, Z. Tong, Y. Wang, G. Li, S. Jin, M. Zhu, T. Zhuang and S.-H. Yu, *Sci. Adv.*, 2023, **9**, eadi9944.
13 M. Schadt, *Annu. Rev. Mater. Res.*, 1997, **27**, 305–379.
14 Y.-H. Kim, Y. Zhai, H. Lu, X. Pan, C. Xiao, E. A. Gaulding, S. P. Harvey, J. J. Berry, Z. V. Vardeny, J. M. Luther and M. C. Beard, *Science*, 2021, **371**, 1129–1133.
15 H. Fan, K. Li, T. Tu, X. Zhu, L. Zhang and M. Liu, *Angew. Chem., Int. Ed.*, 2022, **61**, e202200727.
16 H. Zheng, W. Li, W. Li, X. Wang, Z. Tang, S. X.-A. Zhang and Y. Xu, *Adv. Mater.*, 2018, **30**, 1705948.
17 E. Peeters, M. P. T. Christiaans, R. A. J. Janssen, H. F. M. Schoo, H. P. J. M. Dekkers and E. W. Meijer, *J. Am. Chem. Soc.*, 1997, **119**, 9909–9910.
18 D.-W. Zhang, M. Li and C.-F. Chen, *Chem. Soc. Rev.*, 2020, **49**, 1331–1343.
19 M. Oda, H. G. Nothofer, G. Lieser, U. Scherf, S. C. J. Meskers and D. Neher, *Adv. Mater.*, 2000, **12**, 362–365.
20 D. Di Nuzzo, C. Kulkarni, B. Zhao, E. Smolinsky, F. Tassinari, S. C. J. Meskers, R. Naaman, E. W. Meijer and R. H. Friend, *ACS Nano*, 2017, **11**, 12713–12722.

21 Y. Yang, R. C. da Costa, D.-M. Smilgies, A. J. Campbell and M. J. Fuchter, *Adv. Mater.*, 2013, **25**, 2624–2628.
22 L. Wan, J. Wade, F. Salerno, O. Arteaga, B. Laidlaw, X. Wang, T. Penfold, M. J. Fuchter and A. J. Campbell, *ACS Nano*, 2019, **13**, 8099–8105.
23 M. Wang, K. Yang, X. Wang, Z. A. Tan, K. Pan, J. Deng and B. Zhao, *Adv. Opt. Mater.*, 2024, **12**, 2301513.
24 J. Hong, S. Kim, G. Park, Y. Lee, H. Kim, S. Kim, T.-W. Lee, C. Kim and Y. You, *Chem. Sci.*, 2021, **12**, 8668–8681.
25 M. P. Davydova, L. Meng, M. I. Rakhmanova, Z. Jia, A. S. Berezin, I. Y. Bagryanskaya, Q. Lin, H. Meng and A. V. Artem'ev, *Adv. Mater.*, 2023, **35**, 2303611.
26 Y. Hu, F. Song, Z. Xu, Y. Tu, H. Zhang, Q. Cheng, J. W. Y. Lam, D. Ma and B. Z. Tang, *ACS Appl. Polym. Mater.*, 2019, **1**, 221–229.
27 J.-M. Teng and C.-F. Chen, *ChemPhotoChem*, 2023, e202300253.
28 K.-K. Tan, W.-C. Guo, W.-L. Zhao, M. Li and C.-F. Chen, *Angew. Chem., Int. Ed.*, 2024, e202412283.
29 K. S. Whitehead, M. Grell, D. D. C. Bradley, M. Jandke and P. Strohriegl, *Appl. Phys. Lett.*, 2000, **76**, 2946–2948.
30 M. Oda, H. G. Nothofer, U. Scherf, V. Šunjić, D. Richter, W. Regenstein and D. Neher, *Macromolecules*, 2002, **35**, 6792–6798.
31 Y. Geng, A. Trajkovska, S. W. Culligan, J. J. Ou, H. M. P. Chen, D. Katsis and S. H. Chen, *J. Am. Chem. Soc.*, 2003, **125**, 14032–14038.
32 C. Kulkarni, M. H. C. van Son, D. Di Nuzzo, S. C. J. Meskers, A. R. A. Palmans and E. W. Meijer, *Chem. Mater.*, 2019, **31**, 6633–6641.
33 J. Luo, Z. Xie, J. W. Y. Lam, L. Cheng, H. Chen, C. Qiu, H. S. Kwok, X. Zhan, Y. Liu, D. Zhu and B. Z. Tang, *Chem. Commun.*, 2001, 1740–1741.
34 L. Yang, Y. Zhang, X. Zhang, N. Li, Y. Quan and Y. Cheng, *Chem. Commun.*, 2018, **54**, 9663–9666.
35 Y. Zhang, T. Jing, Y. Quan, S. Ye and Y. Cheng, *Adv. Opt. Mater.*, 2022, **10**, 2200915.
36 T. Imagawa, S. Hirata, K. Totani, T. Watanabe and M. Vacha, *Chem. Commun.*, 2015, **51**, 13268–13271.
37 S. Feuillastre, M. Pauton, L. Gao, A. Desmarchelier, A. J. Riives, D. Prim, D. Tondelier, B. Geffroy, G. Muller, G. Clavier and G. Pieters, *J. Am. Chem. Soc.*, 2016, **138**, 3990–3993.
38 M. Li, Y.-F. Wang, D. Zhang, L. Duan and C.-F. Chen, *Angew. Chem., Int. Ed.*, 2020, **59**, 3500–3504.
39 Y.-F. Wang, M. Li, J.-M. Teng, H.-Y. Zhou, W.-L. Zhao and C.-F. Chen, *Angew. Chem., Int. Ed.*, 2021, **60**, 23619–23624.
40 J.-M. Teng, D.-W. Zhang, Y.-F. Wang and C.-F. Chen, *ACS Appl. Mater. Interfaces*, 2022, **14**, 1578–1586.
41 J.-M. Teng and C.-F. Chen, *Adv. Opt. Mater.*, 2023, **11**, 2300550.
42 W.-L. Zhao, K.-K. Tan, W.-C. Guo, C.-H. Guo, M. Li and C.-F. Chen, *Adv. Sci.*, 2024, **11**, 2309031.
43 F. Liu, Z. Cheng, L. Wan, Z. Feng, H. Liu, H. Jin, L. Gao, P. Lu and W. Yang, *Small*, 2022, **18**, 2106462.
44 T. Hatakeyama, K. Shiren, K. Nakajima, S. Nomura, S. Nakatsuka, K. Kinoshita, J. Ni, Y. Ono and T. Ikuta, *Adv. Mater.*, 2016, **28**, 2777–2781.
45 J.-A. Seo, Y. Im, S. H. Han, C. W. Lee and J. Y. Lee, *ACS Appl. Mater. Interfaces*, 2017, **9**, 37864–37872.
46 G. Kreiza, D. Banevičius, J. Jovaišaitė, S. Juršėnas, T. Javorskis, V. Vaitkevičius, E. Orentas and K. Kazlauskas, *J. Mater. Chem. C*, 2020, **8**, 8560–8566.
47 L. Wu, J. Xu, Z. Zhang, W. Xue, T. Wang, C. Yan, J. He, Y. He, H. Yan and H. Meng, *Mater. Adv.*, 2022, **3**, 1729–1736.
48 J. M. Moreno-Naranjo, F. Furlan, J. Wang, S. T. J. Ryan, T. Matulaitis, Z. Xu, Q. Zhang, L. Minion, M. Di Girolamo, T. Jávorfi, G. Siligardi, J. Wade, N. Gasparini, E. Zysman-Colman and M. J. Fuchter, *Adv. Mater.*, 2024, **36**, 2402194.
49 L. Wan, J. Wade, X. Shi, S. Xu, M. J. Fuchter and A. J. Campbell, *ACS Appl. Mater. Interfaces*, 2020, **12**, 39471–39478.
50 H. Yan, J. Wade, L. Wan, S. Kwon, M. J. Fuchter, A. J. Campbell and J.-S. Kim, *J. Mater. Chem. C*, 2022, **10**, 9512–9520.
51 L. Wan, X. Shi, J. Wade, A. J. Campbell and M. J. Fuchter, *Adv. Opt. Mater.*, 2021, **9**, 2100066.
52 X. Su, Z. Huang, Z. Zhong, F. Peng, T. Guo, L. Hu and L. Ying, *Chem. Phys. Lett.*, 2022, **806**, 140011.
53 L. Wan, J. Wade, X. Wang, A. J. Campbell and M. J. Fuchter, *J. Mater. Chem. C*, 2022, **10**, 5168–5172.
54 X. Zhang, Z. Xu, Y. Zhang, Y. Quan and Y. Cheng, *J. Mater. Chem. C*, 2020, **8**, 15669–15676.
55 X. Zhang, Z. Xu, Y. Zhang, Y. Quan and Y. Cheng, *ACS Appl. Mater. Interfaces*, 2021, **13**, 55420–55427.
56 D.-M. Lee, J.-W. Song, Y.-J. Lee, C.-J. Yu and J.-H. Kim, *Adv. Mater.*, 2017, **29**, 1700907.
57 J.-H. Jung, D.-M. Lee, J.-H. Kim and C.-J. Yu, *J. Mater. Chem. C*, 2018, **6**, 726–730.
58 C.-H. Guo, Y. Zhang, W.-L. Zhao, K.-K. Tan, L. Feng, L. Duan, C.-F. Chen and M. Li, *Adv. Mater.*, 2024, **36**, 2406550.
59 Y. Zhang, Y. Li, Y. Quan, S. Ye and Y. Cheng, *Angew. Chem., Int. Ed.*, 2023, **62**, e202214424.
60 Y. Zhang, D. Li, Q. Li, Y. Quan and Y. Cheng, *Adv. Funct. Mater.*, 2023, **33**, 2309133.
61 Z. Geng, Y. Zhang, Y. Zhang, Y. Li, Y. Quan and Y. Cheng, *J. Mater. Chem. C*, 2021, **9**, 12141–12147.
62 Y. Wang, Y. Li, S. Liu, F. Li, C. Zhu, S. Li and Y. Cheng, *Macromolecules*, 2016, **49**, 5444–5451.
63 Z. Geng, Y. Zhang, Y. Zhang, Y. Quan and Y. Cheng, *Angew. Chem., Int. Ed.*, 2022, **61**, e202202718.
64 K. Baek, D.-M. Lee, Y.-J. Lee, H. Choi, J. Seo, I. Kang, C.-J. Yu and J.-H. Kim, *Light: Sci. Appl.*, 2019, **8**, 120.
65 J. Cheng, F. Ge, Y. Xiang, H. Zhang, Y. Kuai, P. Hou, D. Zhang, L. Qiu, Q. Zhang and G. Zou, *J. Mater. Chem. C*, 2020, **8**, 6521–6527.

